Available online at www.sciencedirect.com
SCIENCE DIRECT®
Physics of the Earth and Planetary Interiors 150 (2005) 45–61
PHYSICS OF THE EARTH AND PLANETARY INTERIORS
www.elsevier.com/locate/pepi

Reciprocity in electromagnetics: application to modelling marine magnetometric resistivity data

Jiuping Chen[a,*], Douglas W. Oldenburg[a], Eldad Haber[b]

[a] *Department of Earth & Ocean Sciences, Geophysical Inversion Facility, University of British Columbia, Vancouver, BC, Canada V6T 1Z4*
[b] *Department of Mathematics & Computer Science, Emory University, Atlanta, GA 30322, USA*

Received 18 July 2003; received in revised form 3 November 2003; accepted 16 August 2004

Abstract

The marine magnetometric resistivity (MMR) can be used to obtain resistivity structure beneath the ocean floor. Because of logistical reasons, many more transmitters than receivers are deployed in a survey. This makes it difficult to carry out 3-D forward modelling of magnetometric resistivity data, since each transmitter source requires a separate solution of Maxwell's equations in order to generate the fields. Two methods are presented to overcome this difficulty. The first is based upon the Lorentz reciprocity theorem. With this theorem, the magnetic field at a receiver, generated by a long vertical electrical bipole, is exactly the same as the normalized electromotive force induced in the transmitter wire generated by an artificial magnetic dipole located at the receiver position. The second is the adjoint method in which the magnetic field can be obtained by solving an adjoint equation with an artificial source at each receiver. We show that these two methods are eventually identical: the artificial source in both methods is a steady current in a loop, and the "measurement" is the voltage along the transmitter wire. However the adjoint algorithm is computationally more efficient and we use it in the 3-D marine MMR forward modelling. We verify the code with a synthetic 3-D example. Use of the reciprocity significantly reduces the computational load, making the practical marine MMR problem tractable.

Keywords: Lorentz reciprocity; Adjoint; Magnetometric resistivity; Electromagnetic induction; Forward modelling; Marine electromagnetics

1. Introduction

The marine magnetometric resistivity (MMR) method is an electromagnetic (EM) exploration method that has been successfully used for investigation of electrical resistivity structures of the seafloor (Chave et al., 1991). The geometry of the system is shown in Fig. 1, which is an adaptation of terrestrial MMR approaches (Edwards et al., 1985). The method essentially involves measurement of magnetic fields associated with man-made, non-inductive (low-frequency or pseudo-DC) current flow energized into the seawa-

* Corresponding author. Tel.: +1 604 822 4180; fax: +1 604 822 6088.
E-mail address: jchen@eos.ubc.ca (J. Chen).

0031-9201/$ – see front matter © 2004 Elsevier B.V. All rights reserved.
doi:10.1016/j.pepi.2004.08.015

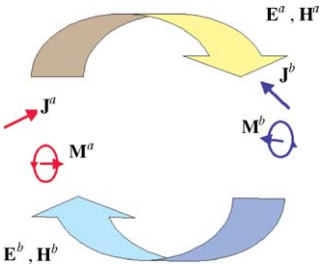

Fig. 1. A schematic illustrating the reciprocity relationship between a transmitter source **a** and a receiver source **b**.

ter and seafloor through two vertically separated electrodes. The magnetic field measured at the ocean bottom magnetometer depends on the total current entering the seafloor through an Ampère circuit centered on the source and passing through the receiver. In the presence of a layered seafloor, the magnetic field generated by the bipole source possesses an azimuthal symmetry, and the bulk resistivity of the seafloor can be estimated from the amplitude of the magnetic field, given that the current transmitted is known. For general 3-D resistivity structures beneath the seafloor we have to resort to a numerical algorithm (Chen et al., 2002) for both forward modelling and inversion.

A unique characteristic of the marine MMR lies in the reality that there are many more transmitter sources than receivers. In the Juan de Fuca Ridge example (Evans et al., 1998), 34 transmitter sources were deployed while there were only three receivers. This is in contrast to the terrestrial situation, in which only a few (sometimes one!) transmitters are deployed. In a recent MMR experiment in the Eastern Pacific Rise (Evans and Webb, 2002), more than 200 source bipoles were used and 10 three-component magnetometers were placed on the seafloor. From a numerical perspective, this makes it difficult to carry out 3-D forward modelling and inversion of marine MMR data, since each transmitter source requires a separate solution of Maxwell's equations in order to generate the fields.

This difficulty motivated us first to consider applying the Lorentz reciprocity theorem to reduce the heavy computational load. According to the reciprocity theorem, in its simplest sense, a response of a system to a source is unchanged when source and receiver are interchanged (Harrington, 1961). By response, we do not necessarily mean the electric or magnetic field. In Parasnis's tutorial (1988), a response might be a voltage or complex electromotive force (emf) developed in a receiver. In principle, invoking reciprocity can greatly reduce the computations. If the number of receivers is N_{rx}, and three components of magnetic field are measured, we only need to put $3N_{rx}$ artificial magnetic dipole (or current loop) sources at N_{rx} receiver locations (x-, y-, and z-oriented in turn at one receiver location), regardless of the original number of transmitters. In the EPR experiment mentioned above, instead of working with 200 transmitters in forward modelling, we need only 30 artificial sources, or, 20 if only x- and y-components are used. This reduces the forward modelling computations by an order of magnitude.

The adjoint method, originally defined by Lagrange, has since been thoroughly substantiated and broadly applied in solving many problems (e.g., Marchuk et al., 1996). A common usage in EM investigation is to use the adjoint method to compute the sensitivity (e.g., Weidelt, 1975; Madden, 1990; McGillivray et al., 1994). In this paper, we use the adjoint method to reformulate our 3-D MMR forward modelling. Interestingly, we can find similarities in terms of computational load and "physical" meaning between the Lorentz reciprocity and the adjoint method. As a matter of fact, the adjoint field is closely related to electromagnetic migration field, which was introduced by Zhdanov et al. Interested readers can refer to their work (e.g. Zhdanov and Frenkel, 1983; Zhdanov et al., 1996; Zhdanov, 2002), and to time reversal methods (Borcea et al., 2002). In fact, migration techniques and their derivation relay on the properties of the adjoint equation. Our intention here is to specifically analyze the adjoint of the MMR experiment and its use.

In our opinion the relationship between Lorentz reciprocity and the adjoint method deserves further investigation. Although Lorentz reciprocity is physically realizable (we can set out physical instruments to generate and measure the fields), and the adjoint is a mathematical tool, we find that the underlying physical ideas are identical and the two approaches produce the same numerical solution. For the MMR problem, this intimate relation can be revealed by: (1) investigating the low-frequency characteristic of the electric field due to a magnetic dipole in a general 3-D medium; (2) numerically implementing the adjoint algorithm, in which the artificial source for the adjoint equation is exactly equivalent to a magnetic dipole, but with a frequency of zero; (3) examining the inner product in the adjoint

method to show that it is equivalent to producing a voltage difference along the transmitter wire.

In this paper, we first briefly outline Lorentz reciprocity, and provide a reciprocal representation for MMR. Then we discuss the electromagnetic adjoint method for zero frequency in terms of functions and discrete operators. We show how to implement the adjoint algorithm in the forward modelling, and validate the code with a synthetic example. The paper concludes with a discussion.

2. Lorentz reciprocity method

2.1. The Lorentz reciprocity theorem

In a medium which is characterized by a variable electrical permittivity ϵ, a variable magnetic permeability μ, and a variable conductivity σ, Maxwell's equations in the frequency domain become (assuming a harmonic time dependence $e^{i\omega t}$)

$$\nabla \times \boldsymbol{E} = -i\omega\mu \boldsymbol{H} + \boldsymbol{M}, \tag{1}$$

$$\nabla \times \boldsymbol{H} = (\sigma + i\omega\epsilon)\boldsymbol{E} + \boldsymbol{J}, \tag{2}$$

where $\boldsymbol{J}$ and $\boldsymbol{M}$ are imposed electric and magnetic current densities. For a magnetic source located at $\boldsymbol{r}_{tx}$, if the magnetic moment is $\boldsymbol{m}$, then $\boldsymbol{M} = i\omega\mu\boldsymbol{m}\delta(\boldsymbol{r} - \boldsymbol{r}_{tx})$. Consider two sets of exciting sources $\boldsymbol{J}^{\mathrm{a}}$, $\boldsymbol{M}^{\mathrm{a}}$ and $\boldsymbol{J}^{\mathrm{b}}$, $\boldsymbol{M}^{\mathrm{b}}$. Denote the fields produced by the **a** source as $\boldsymbol{E}^{\mathrm{a}}$ and $\boldsymbol{H}^{\mathrm{a}}$, and the fields produced by the **b** source as $\boldsymbol{E}^{\mathrm{b}}$ and $\boldsymbol{H}^{\mathrm{b}}$. With simple arithmetic manipulations and use of vector identities,

$$\nabla \cdot (\boldsymbol{E}^{\mathrm{a}} \times \boldsymbol{H}^{\mathrm{b}} - \boldsymbol{E}^{\mathrm{b}} \times \boldsymbol{H}^{\mathrm{a}}) = \boldsymbol{E}^{\mathrm{b}} \cdot \boldsymbol{J}^{\mathrm{a}} - \boldsymbol{H}^{\mathrm{a}} \cdot \boldsymbol{M}^{\mathrm{b}} + \boldsymbol{E}^{\mathrm{a}} \cdot \boldsymbol{J}^{\mathrm{b}} + \boldsymbol{H}^{\mathrm{b}} \cdot \boldsymbol{M}^{\mathrm{a}}. \tag{3}$$

At points where there is source-free ($\boldsymbol{J} = \boldsymbol{M} = 0$), Eq. (3) will be

$$\nabla \cdot (\boldsymbol{E}^{\mathrm{a}} \times \boldsymbol{H}^{\mathrm{b}} - \boldsymbol{E}^{\mathrm{b}} \times \boldsymbol{H}^{\mathrm{a}}) = 0. \tag{4}$$

This is called the *Lorentz reciprocity theorem* (Harrington, 1961). Eq. (3) can be integrated over all space. When all sources and the medium are of finite extent, the left-hand side of Eq. (3), evaluated via the divergence theorem, goes to zero because the electric and magnetic fields approach zero in accordance with the radiation boundary condition. As a consequence,

$$\int\int\int_v (\boldsymbol{E}^{\mathrm{a}} \cdot \boldsymbol{J}^{\mathrm{b}} + \boldsymbol{H}^{\mathrm{a}} \cdot \boldsymbol{M}^{\mathrm{b}})\,\mathrm{d}v = \int\int\int_v (\boldsymbol{E}^{\mathrm{b}} \cdot \boldsymbol{J}^{\mathrm{a}} + \boldsymbol{H}^{\mathrm{b}} \cdot \boldsymbol{M}^{\mathrm{a}})\,\mathrm{d}v. \tag{5}$$

This is the most useful form of the reciprocity theorem for our purpose. The only assumption made is that the medium is linear, which means the electric current density, magnetic current density and electric displacement are linear functions of electric and magnetic field intensities (Parasnis, 1988).

As sketched in Fig. 1, we can regard location **a** as a transmitter source location, and **b** as a receiver location. From Eq. (5), in very general terms, reciprocity states that the response in the new system remains the same as in the old one if the transmitter and receiver are interchanged. As pointed out by Parasnis (1988), reciprocity does not mean to exchange transmitter and receiver in terms of their respective orientations or positions in space. Instead, the reciprocal of the transmitter is obtained by replacing the transmitter with a measuring device, called as "voltmeter", and the receiver is replaced with a current-generating device, called as "generator". In the EM geophysics, reciprocity may have four different representations, depending upon the transmitter source and the field measured (Appendix A).

2.2. Representation for MMR

The MMR method belongs to the second category in Appendix A, i.e., the transmitter is a grounded wire and the magnetic field is measured. Assume the transmitter wire is located at position a and the receiver at b. Setting-up the electric and magnetic current densities at both locations and substituting them into Eq. (5), yields

$$\boldsymbol{B}^{\mathrm{a}} = \frac{\hat{\boldsymbol{u}} I^{\mathrm{a}}}{i\omega I^{\mathrm{a}} s^{\mathrm{a}}} \int_{l_{\mathrm{a}}} \boldsymbol{E}^{\mathrm{b}} \cdot d\boldsymbol{l}_{\mathrm{a}}, \tag{6}$$

where $\boldsymbol{B}^{\mathrm{a}}$ is the magnetic field at receiver location b, due to the transmitter wire with current strength I^{a} and wire length l_{a}; $\boldsymbol{E}^{\mathrm{b}}$ is electric field at a location along the transmitter wire, due to an artificial magnetic dipole (or small current loop), located at the receiver position and ω is the angular frequency in the magnetic dipole. The magnetic moment of the artificial dipole is represented

by

$$\boldsymbol{m}^{\mathrm{b}} = \hat{\boldsymbol{u}} I^{\mathrm{b}} s^{\mathrm{b}}, \tag{7}$$

where $\hat{\boldsymbol{u}}$ is the unit vector normal to the loop area and is in the direction of the right-hand thumb if the fingers of the right-hand are curled in the direction of the current I^b circulating in the loop (right-hand rule), and s^{b} is the area of the small loop.

Eq. (6) is the fundamental expression of reciprocity for the MMR problem. It clearly shows that the magnetic field at a receiver location due to a transmitter wire source can be obtained by an integration of an artificial $\boldsymbol{E}^{\mathrm{b}}$ field along the transmitter wire, then normalized by a factor related to angular frequency ω, current I^{a}, and magnetic moment m^{b}. The artificial $\boldsymbol{E}^{\mathrm{b}}$ field is generated by an artificial current loop source (or magnetic dipole) located at the receiver position. Since the magnetic field measured in MMR is almost galvanic, the frequency involved must be very low, say less than 0.001 Hz. In order to use this reciprocal expression, it should be noted that the magnetic dipole source must be in the same direction as the recorded magnetic field. If only the x-component of magnetic field is required, an x-oriented magnetic dipole must be located at the receiver position. If three components are to be computed, we successively put three magnetic dipoles in the x-, y-, and z-directions.

In the marine MMR situation, generally the transmitter wire is vertical. This means we only need integrate E_z along the wire. Also, for simplicity, we can assume $I^{\mathrm{a}} = 1$ and use a unit magnetic dipole ($I^{\mathrm{b}} s^{\mathrm{b}} = 1$). By doing so, the above expression (6) can be simplified as

$$B_k = \lim_{\omega \to 0} \frac{1}{i\omega} \int_0^H E_z^k \, \mathrm{d}z, \tag{8}$$

where H is the length of the wire or thickness of seawater; the superscript k (= x, y, or z) at E_z^k denotes the orientation of the magnetic dipole, and the subscript k in B_k represents the corresponding magnetic component.

At first sight the division by $i\omega$ seems to pose a problem because $\omega \to 0$. However, for low frequency it can be shown that $E(\omega) = i\omega F$, where F is a real number and independent of frequency (see Appendix B). Therefore, the $i\omega$ term in the denominator is cancelled and Eq. (8), is therefore, a stable solution for calculating the magnetic field using reciprocity. We carried out numerical tests in 1-D to validate the applicability of Eq. (8). Details can be found in Appendix C.

These simple numerical tests show that we can compute the magnetic field due to a grounded wire indirectly by using the reciprocity representation. However, use of the reciprocity requires us to develop a 3-D EM forward modelling code in frequency-domain with a loop source. This is not an easy task, and in fact is more computational demanding than the MMR problem itself. Furthermore, the division by a small frequency can be numerically unstable. Therefore, we turn to the adjoint equation method.

3. Adjoint equation method

We can also derive the reciprocal relation between the magnetic field due to a grounded wire and electrical field due to an artificial magnetic dipole through use of the adjoint operator. This methodology is also frequently used to compute sensitivities (Dorn et al., 1999; Mackie and Madden, 1993; Zhdanov, 2002). To show how the adjoint analysis can be used we use the notation from Dorn et al. (1999) and work at zero frequency with functional notation.

3.1. Continuous adjoint analysis

If we set the frequency to zero, then Eqs. (1) and (2) can be written as

$$\begin{pmatrix} -\sigma & \nabla\times \\ \nabla\times & 0 \end{pmatrix} \begin{pmatrix} \boldsymbol{E} \\ \boldsymbol{H} \end{pmatrix} = \begin{pmatrix} \boldsymbol{J} \\ \boldsymbol{M} \end{pmatrix} \tag{9}$$

or

$$\mathcal{A}_{\mathrm{dc}} \cdot \begin{pmatrix} \boldsymbol{E} \\ \boldsymbol{H} \end{pmatrix} = \begin{pmatrix} \boldsymbol{J} \\ \boldsymbol{M} \end{pmatrix}. \tag{10}$$

where $\mathcal{A}_{\mathrm{dc}}$ is defined as

$$\mathcal{A}_{\mathrm{dc}} = \begin{pmatrix} -\sigma & \nabla\times \\ \nabla\times & 0 \end{pmatrix}. \tag{11}$$

A magnetic field value B_k ($k = x$, y, or z) at position $\boldsymbol{r}_{rx}$ is

$$B_k(\boldsymbol{r}_{rx}) = \mu \int_v \boldsymbol{H}(\boldsymbol{r}) \cdot \boldsymbol{e}_k \delta(\boldsymbol{r} - \boldsymbol{r}_{rx}) \, \mathrm{d}v, \tag{12}$$

where $\boldsymbol{e}_k$ is a unit vector pointing to k direction. Our goal is to write Eq. (12) as an inner product that allows us to calculate B_k.

Suppose $\boldsymbol{w}$ and $\boldsymbol{v}$ belong to a linear space (a complex Hilbert space of vector functions determined in domain Ω), equipped with an inner product given by

$$\langle \boldsymbol{w}, \boldsymbol{v} \rangle = \int_{\Omega} \boldsymbol{w} \cdot \overline{\boldsymbol{v}} \, \mathrm{d}\Omega, \tag{13}$$

where $\overline{\boldsymbol{v}}$ is the complex conjugate of $\boldsymbol{v}$. Let $\boldsymbol{L}$ be a bounded and linear operator, then its adjoint $\boldsymbol{L}^*$ (Hermitian adjoint) is defined as an operator that satisfies

$$\langle \boldsymbol{L}\boldsymbol{w}, \boldsymbol{v} \rangle = \langle \boldsymbol{w}, \boldsymbol{L}^* \boldsymbol{v} \rangle. \tag{14}$$

Following Dorn et al. (1999), Eq. (12) can be expanded as

$$B_k(\boldsymbol{r}_{rx}) = \mu \left\langle \begin{pmatrix} \boldsymbol{E} \\ \boldsymbol{H} \end{pmatrix}, \begin{pmatrix} \boldsymbol{0} \\ \delta(\boldsymbol{r} - \boldsymbol{r}_{rx})\boldsymbol{e}_k \end{pmatrix} \right\rangle$$

$$= \mu \left\langle \mathcal{A}_{\mathrm{dc}}^{-1} \begin{pmatrix} \boldsymbol{J} \\ \boldsymbol{M} \end{pmatrix}, \begin{pmatrix} \boldsymbol{0} \\ \delta(\boldsymbol{r} - \boldsymbol{r}_{rx})\boldsymbol{e}_k \end{pmatrix} \right\rangle \tag{15}$$

$$= \mu \left\langle \begin{pmatrix} \boldsymbol{J} \\ \boldsymbol{M} \end{pmatrix}, (\mathcal{A}_{\mathrm{dc}}^*)^{-1} \begin{pmatrix} \boldsymbol{0} \\ \delta(\boldsymbol{r} - \boldsymbol{r}_{rx})\boldsymbol{e}_k \end{pmatrix} \right\rangle, \tag{16}$$

where $\mathcal{A}_{\mathrm{dc}}^*$ is the adjoint of $\mathcal{A}_{\mathrm{dc}}$,

$$\mathcal{A}_{\mathrm{dc}}^* = \begin{pmatrix} -\sigma & \nabla\times \\ \nabla\times & 0 \end{pmatrix} \tag{17}$$

So $\mathcal{A}_{\mathrm{dc}}^* \equiv \mathcal{A}_{\mathrm{dc}}$, the adjoint operator is the same as the forward operator (self-adjoint). The second operation in Eq. (15) is equivalent to solving the *adjoint equation*

$$\mathcal{A}_{\mathrm{dc}}^* \cdot \begin{pmatrix} \boldsymbol{E}^{\mathrm{adj}} \\ \boldsymbol{H}^{\mathrm{adj}} \end{pmatrix} = \begin{pmatrix} -\sigma & \nabla\times \\ \nabla\times & 0 \end{pmatrix} \begin{pmatrix} \boldsymbol{E}^{\mathrm{adj}} \\ \boldsymbol{H}^{\mathrm{adj}} \end{pmatrix}$$

$$= \begin{pmatrix} \boldsymbol{0} \\ \delta(\boldsymbol{r} - \boldsymbol{r}_{rx})\boldsymbol{e}_k \end{pmatrix} \tag{18}$$

Since $\boldsymbol{M} = \boldsymbol{0}$ in the MMR, we end up with the following relation

$$B_k(\boldsymbol{r}_{rx}) = \mu \left\langle \begin{pmatrix} \boldsymbol{J} \\ \boldsymbol{0} \end{pmatrix}, \begin{pmatrix} \boldsymbol{E}^{\mathrm{adj}} \\ \boldsymbol{H}^{\mathrm{adj}} \end{pmatrix} \right\rangle$$

$$= \mu \int_v \boldsymbol{J} \cdot \overline{\boldsymbol{E}^{\mathrm{adj}}} \, \mathrm{d}v = \mu \int_0^H \overline{E_z^{\mathrm{adj}}} \, \mathrm{d}z, \tag{19}$$

where H is the length of the vertical transmitter wire. Because $\mathcal{A}_{\mathrm{dc}}^*$ is real and self-adjoint,

$$B_k(\boldsymbol{r}_{rx}) = \mu \int_0^H E_z^{\mathrm{adj}} \, \mathrm{d}z, \tag{20}$$

where $\boldsymbol{E}^{\mathrm{adj}}$ is the solution of Eq. (18). So we may numerically solve

$$\nabla \times \boldsymbol{E}^{\mathrm{adj}} = \boldsymbol{e}_k \delta(\boldsymbol{r} - \boldsymbol{r}_{rx}), \tag{21}$$

$$\nabla \times \boldsymbol{H}^{\mathrm{adj}} = \sigma \boldsymbol{E}^{\mathrm{adj}}, \tag{22}$$

to obtain the adjoint electric field.

The above equations are formulated in terms of $\boldsymbol{E}$ and $\boldsymbol{H}$. However, these equations do not have a unique solution due to the null space of the *curl* and this may generate difficulties when a numerical solution is calculated. It is, therefore, convenient to develop a similar relation using the potentials (Haber et al., 2000).

As shown in Fig. 2, suppose an exciting current is impressed into the seawater and seafloor through a wire and a pair of electrodes. The current flow, in the wire, seawater, and in the seafloor, gives rise to a magnetic field. This magnetic field can be measured by an ocean bottom magnetometer (OBM) located at the seafloor. If the frequency in the transmitter current waveform is sufficiently low so that the inductive effect can be ignored, then the electric field $\boldsymbol{E}$ and magnetic field $\boldsymbol{H}$ satisfy

$$\nabla \times \boldsymbol{E} = 0, \tag{23}$$

$$\nabla \times \boldsymbol{H} - \sigma \boldsymbol{E} = \boldsymbol{J}^{\mathrm{s}}, \tag{24}$$

$$\nabla \cdot (\mu \boldsymbol{H}) = 0, \tag{25}$$

where $\boldsymbol{J}^{\mathrm{s}}$ is the impressed electric current density in the wire in A/m^2. We define a scalar potential ϕ and a vector potential $\boldsymbol{A}$ such that

$$\boldsymbol{E} = -\nabla\phi, \tag{26}$$

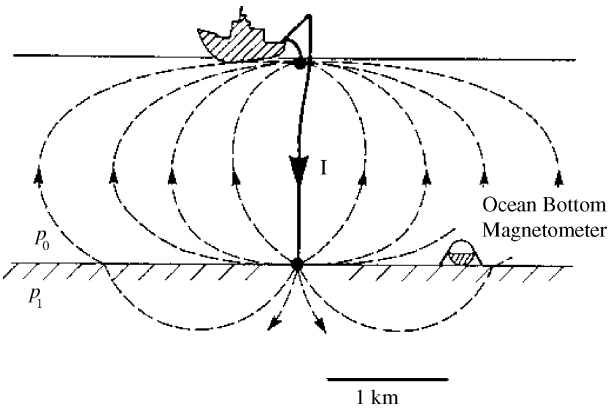

Fig. 2. A schematic of the marine MMR method which shows a vertical bipole source of current and an ocean bottom magnetometer (from Edwards and Nabighian, 1991).

and

$$\boldsymbol{H} = \frac{1}{\mu}\nabla \times \boldsymbol{A}. \tag{27}$$

In addition, the Coulomb gauge condition is imposed on $\boldsymbol{A}$, i.e., $\nabla \cdot \boldsymbol{A} = 0$. Then ϕ and $\boldsymbol{A}$ satisfy

$$\nabla \cdot \sigma \nabla \phi = \nabla \cdot \boldsymbol{J}^{\mathrm{s}}, \tag{28}$$

and

$$\nabla \times \frac{1}{\mu}\nabla \times \boldsymbol{A} + \sigma \nabla \phi = \boldsymbol{J}^{\mathrm{s}}. \tag{29}$$

Putting these two equations together, we have a system

$$\begin{pmatrix} \nabla \times \mu^{-1}\nabla \times & -\nabla\mu^{-1}\nabla\cdot & \sigma\nabla \\ & 0 & \nabla\cdot\sigma\nabla \end{pmatrix} \begin{pmatrix} \boldsymbol{A} \\ \phi \end{pmatrix} = \begin{pmatrix} \boldsymbol{J}^{\mathrm{s}} \\ \nabla \cdot \boldsymbol{J}^{\mathrm{s}} \end{pmatrix}, \tag{30}$$

where the second term $-\nabla\mu^{-1}\nabla\cdot$ in the first entry serves as a stabilizer (Haber and Ascher, 2001; Jin, 1993). This quantity is theoretically zero because of the Coulomb gauge. Its inclusion ensures that in the discrete formulation, that the first element in the matrix behaves as a Laplacian.

In this case the forward operator for the potentials is

$$\mathcal{A} = \begin{pmatrix} \nabla \times \mu^{-1}\nabla \times & -\nabla\mu^{-1}\nabla\cdot & \sigma\nabla \\ & 0 & \nabla\cdot\sigma\nabla \end{pmatrix} \tag{31}$$

Unlike the formulation in terms of $\boldsymbol{E}$ and $\boldsymbol{H}$ (see Eq. (17)) the forward operator is not self-adjoint. The diagonal operators are (assuming appropriate boundary conditions), but the adjoint of a gradient is a divergence. The adjoint operator for the $\boldsymbol{A}, \phi$ equations is

$$\mathcal{A}^* = \begin{pmatrix} \nabla \times \mu^{-1}\nabla \times & -\nabla\mu^{-1}\nabla\cdot & 0 \\ & -\nabla\cdot\sigma & \nabla\cdot\sigma\nabla \end{pmatrix} \tag{32}$$

Unlike the original operator which is not invertible for electric and magnetic fields, this operator is well defined and invertible. Before discussing the discrete adjoint equation using potentials, we present the discrete forward modelling.

3.2. Discrete forward problem

In order to obtain a numerical solution, the 3-D medium is discretized into a large number of rectangular cells whose conductivity and magnetic permeability value are constant. A finite-volume method on a staggered grid (Chen et al., 2002; Haber et al., 2000) is used to generate the matrix equation. $\boldsymbol{A}$ and current density $\boldsymbol{J}$ are defined at centers of cell faces, $\boldsymbol{H}$ at centers of cell edges, and ϕ at cell centers. Eqs. (28) and (29) become

$$\begin{pmatrix} \nabla_{\mathrm{h}}^{(\mathrm{e})} \times \boldsymbol{M}_{\mathrm{e}}^{-1}\nabla_{\mathrm{h}}^{(\mathrm{f})} \times & -\nabla_{\mathrm{h}}\boldsymbol{M}_{\mathrm{c}}^{-1}\nabla_{\mathrm{h}}\cdot & \boldsymbol{S}\nabla_{\mathrm{h}} \\ & 0 & \nabla_{\mathrm{h}}\cdot\boldsymbol{S}\nabla_{\mathrm{h}} \end{pmatrix} \begin{pmatrix} \boldsymbol{A} \\ \phi \end{pmatrix} = \begin{pmatrix} \boldsymbol{J}^{\mathrm{s}} \\ \nabla_{\mathrm{h}} \cdot \boldsymbol{J} \end{pmatrix} \tag{33}$$

where the matrices $\nabla_{\mathrm{h}}^{(\mathrm{e})}\times$ and $\nabla_{\mathrm{h}}^{(\mathrm{f})}\times$ are assembled from the discretization of the ***curl*** operator, projecting from cell edges to faces and from faces to edges, respectively; matrices $\nabla_{\mathrm{h}}\cdot$ and ∇_{h} correspond to the discretization of the ***div*** and ***grad*** operators. When assembling the discrete first-order partial differential equations, the normal components of $\boldsymbol{A}$ and $\boldsymbol{J}$, and the tangential components of $\boldsymbol{H}$ on the outer boundaries are set to 0. The material matrix $\boldsymbol{S}$ arises from the discretization of the conductivity σ, a harmonic averaging of values at cell faces. The matrices $\boldsymbol{M}_{\mathrm{e}}$ and $\boldsymbol{M}_{\mathrm{c}}$ result from an arithmetic averaging of permeability μ at cell edges and the permeability itself at the cell centers, respectively. The superscript -1 represents the inverse of the matrix. The second term $-\nabla_{\mathrm{h}}\boldsymbol{M}_{\mathrm{c}}^{-1}\nabla_{\mathrm{h}}\cdot$ in the first entry is the discretized stabilizer.

Eq. (33) can be simplified as

$$\mathcal{A}\boldsymbol{u} = s, \tag{34}$$

and its solution can be symbolically written as

$$\boldsymbol{u} = \mathcal{A}^{-1}\boldsymbol{s}, \tag{35}$$

where $\mathcal{A}$ denotes the coefficient matrix and $\mathcal{A}^{-1}$ is its inverse, the vector $\boldsymbol{u} = \begin{pmatrix} A \\ \phi \end{pmatrix}$, and the source vector $\boldsymbol{s} = \begin{pmatrix} \boldsymbol{J}^{\mathrm{s}} \\ \nabla_{\mathrm{h}} \cdot \boldsymbol{J}^{\mathrm{s}} \end{pmatrix}$. The magnetic induction data (or the marine MMR data as called below) at receiver locations can also be represented as

$$\boldsymbol{B} = Qu, \tag{36}$$

where $\boldsymbol{Q}$ is a matrix that extracts the magnetic field at observation sites from the potentials. From Eq. (27), it is easy to see that $\boldsymbol{Q}$ involves *curl* operations and linear interpolation, and therefore is independent of conductivity structure.

3.3. Discrete adjoint equation

In the proceeding Section 2, we derived the discrete matrix form for forward modelling of MMR response. Here we want to show how to directly use the adjoint method to compute the magnetic field. We look at one component of the data at one receiver location for a wire source. We refer to this as the primal datum, to distinguish it from the adjoint datum obtained by using the adjoint method. From Eq. (36), the projection matrix ($\boldsymbol{Q}$) becomes a vector, denoted by $\boldsymbol{q}$. Using Eq. (35), the primal datum, B_k can be represented as

$$B_k = \boldsymbol{q}^{\mathrm{T}}\boldsymbol{u} = \langle \boldsymbol{u}, \boldsymbol{q}\rangle = \left\langle \mathcal{A}^{-1}\boldsymbol{s}, \boldsymbol{q}\right\rangle, \tag{37}$$

where $\boldsymbol{s}$ is the source term given by Eq. (33). Since the adjoint of a real matrix is its transpose, we have

$$B_k = \left\langle \mathcal{A}^{-1}\boldsymbol{s}, \boldsymbol{q}\right\rangle = \left\langle \boldsymbol{s}, (\mathcal{A}^{-1})^{*}\boldsymbol{q}\right\rangle = \left\langle \boldsymbol{s}, (\mathcal{A}^{-1})^{\mathrm{T}}\boldsymbol{q}\right\rangle. \tag{38}$$

Note the difference between the vectors $\boldsymbol{q}$ and $\boldsymbol{s}$ on each side in above equation. On the left-hand side, the vector $\boldsymbol{s}$ is a source, and $\boldsymbol{q}$ is a projection, while on the right-hand side $\boldsymbol{q}$ is equivalent to a source, and $\boldsymbol{s}$ is equivalent to a projection. This is more evident if we re-arrange the right-hand side, and represent the adjoint data by B_{adj},

$$\begin{aligned} B_{\mathrm{adj}} &= \left\langle \boldsymbol{s}, (\mathcal{A}^{-1})^{\mathrm{T}}\boldsymbol{q}\right\rangle = \left\langle \boldsymbol{s}, (\mathcal{A}^{\mathrm{T}})^{-1}\boldsymbol{q}\right\rangle \\ &= \boldsymbol{s}^{\mathrm{T}}(\mathcal{A}^{\mathrm{T}})^{-1}\boldsymbol{q} = \boldsymbol{s}^{\mathrm{T}}\boldsymbol{u}_{\mathrm{adj}}, \end{aligned} \tag{39}$$

where adjoint potential vector $\boldsymbol{u}_{\mathrm{adj}}$ is given by

$$(\mathcal{A}^{T})^{-1}\boldsymbol{q} = \boldsymbol{u}_{\mathrm{adj}}, \tag{40}$$

or equivalently,

$$\mathcal{A}^{\mathrm{T}}\boldsymbol{u}_{\mathrm{adj}} = \boldsymbol{q}. \tag{41}$$

So the magnetic field calculated via the adjoint method is obtained by first solving Eq. (41) for $\boldsymbol{u}_{\mathrm{adj}}$ and then computing an inner product with the real source $\boldsymbol{s}$ as per Eq. (39). This means that we can directly work on the discrete coefficient matrix $\mathcal{A}$, and the source term s obtained in the MMR forward modelling, and do not need to worry about the $i\omega$ term, as encountered in the Lorentz reciprocity.

As shown in Madden (1990), only the transpose of $\nabla\times\nabla\times$ operator is self-adjoint, but not *grad* and *div*. This means $\mathcal{A}$ is not self-adjoint, and $\mathcal{A}^{\mathrm{T}}$ will present a different "physical" problem. The artificial source term $\boldsymbol{q}$ for the adjoint problem in Eq. (41) can be split into two vectors, i.e., $\boldsymbol{q} = [\boldsymbol{q}_A; \boldsymbol{q}_\phi]$. They correspond to the sources for generating the adjoint potentials $\boldsymbol{A}_{\mathrm{adj}}$ and ϕ_{adj}. As can be seen in Section 5.2, $\boldsymbol{q}_\phi = \boldsymbol{0}$. Using Eqs.

(32) and (41), we have

$$\nabla \times \frac{1}{\mu} \nabla \times \boldsymbol{A}_{\mathrm{adj}} = \boldsymbol{q}_A, \tag{42}$$

and

$$\nabla \cdot \sigma \nabla \phi_{\mathrm{adj}} = \nabla \cdot \sigma \boldsymbol{A}_{\mathrm{adj}}. \tag{43}$$

Note in the adjoint problem, we first solve the adjoint potential $\boldsymbol{A}_{\mathrm{adj}}$ from Eq. (42), and then substitute it into the right-hand side of Eq. (43), to eventually solve for potential ϕ_{adj}. This means that $\boldsymbol{A}_{\mathrm{adj}}$ serves as a "source" for producing potential ϕ_{adj}. This, of course, is not a real physical reality, rather it is a mathematical representation.

4. Relationship between reciprocity and adjoint

Two different methods have been discussed to produce the magnetic field in the marine MMR problem. In the Lorentz reciprocity method, we need an artificial magnetic dipole as a source, and we measure the potential difference along the transmitter wire. This potential difference has to be normalized by a term $i\omega$, and we have to mathematically take the limitation when $\omega \longrightarrow 0$, because MMR is a static problem. In the adjoint method, we know that some kind of "source" (vector $\boldsymbol{q}$ in Eq. (41)) is involved, and the adjoint B_{adj} field is the inner product (or summation) of the real source vector $\boldsymbol{s}$, which is related to the transmitter wire, and adjoint potentials. However, the exact physical meanings of the adjoint source $\boldsymbol{q}$ and inner product remain unknown. Further investigation reveals the relationship between these two methods.

We still use the above one component example, and assume the component is B_x. From Eq. (37), we know

$$B_x = \boldsymbol{q}^{\mathrm{T}} \boldsymbol{u} = \boldsymbol{q}^{\mathrm{T}} \begin{pmatrix} \boldsymbol{A} \\ \phi \end{pmatrix} = \boldsymbol{q}_A^{\mathrm{T}} \boldsymbol{A} + \boldsymbol{q}_\phi^{\mathrm{T}} \phi. \tag{44}$$

At the same time, we also know

$$B_x = (\nabla \times \boldsymbol{A})_x = \frac{\partial A_z}{\partial y} - \frac{\partial A_y}{\partial z}. \tag{45}$$

When discretizing the first derivative by finite-difference, B_x in Eq. (44) can be written as a product of two discrete vectors

$$B_x = \frac{1}{h} \begin{pmatrix} 0 \\ \vdots \\ 0 \\ \cdots \\ \vdots \\ +1 \\ \vdots \\ 0 \\ \vdots \\ -1 \\ \vdots \\ \cdots \\ \vdots \\ -1 \\ \vdots \\ 0 \\ \vdots \\ +1 \\ \vdots \end{pmatrix}^{\mathrm{T}} \begin{pmatrix} A_x \\ A_y \\ A_z \end{pmatrix} \tag{46}$$

where h is the length of the cells (suppose uniformly discretized, without loss of generality), and only four entries are not zero in the neighboring vector. Comparing Eq. (44) with (46), it is evident that $\boldsymbol{q}_\phi = \boldsymbol{0}$, and

$$\boldsymbol{q}_A^{\mathrm{T}} = \frac{1}{h}(0 \ldots 0, 0 \cdots + 1 \ldots 0 \cdots - 1 \ldots 0, 0 \cdots - 1 \ldots 0 \cdots + 1 \ldots 0). \tag{47}$$

In Eq. (42), $\boldsymbol{q}_A$ is the "source" for generating the adjoint potential $\boldsymbol{A}_{adj}$. This source should have the property of current density, since Eq. (42) is equivalent to the Ampere's law, i.e., $\nabla \times \boldsymbol{H} = \boldsymbol{J}$. This means $\boldsymbol{q}_A$ is the discretizing vector of a current source, which is exactly the same as a current loop source with current strength of h (the magnetic moment is h^3), as shown in Fig. 3. This demonstrates that the source in the adjoint method is indeed a x-oriented magnetic dipole with a static current.

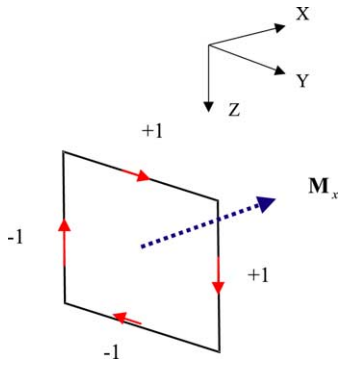

Fig. 3. Vector $\boldsymbol{q}_A$ in the adjoint equation is equivalent to a discretized vector of a current loop, with a magnetic moment pointing to $+x$-direction.

Next we want to see the physical meaning of the inner product of vector $\boldsymbol{s}$ and adjoint vector potential $\boldsymbol{u}_{\text{adj}}$ in the adjoint method. From Eq. (33), the source vector is

$$\boldsymbol{s} = \begin{pmatrix} \boldsymbol{J}^{\text{s}} \\ \nabla_{\text{h}} \cdot \boldsymbol{J}^{\text{s}} \end{pmatrix} \tag{48}$$

After discretization, the sub-vector corresponding to $\boldsymbol{J}^{\text{s}}$ is

$$\boldsymbol{s}_J = \frac{1}{h^2}(0\ldots, 0\ldots, 0\ldots 1\ldots 1\ldots 0)^{\text{T}}, \tag{49}$$

where the ones are the entries for the cells at which the vertical wire goes through; the sub-vector corresponding to $\nabla_{\text{h}} \cdot \boldsymbol{J}^{\text{s}}$ has only two non-zero entries (equivalent to the two electrodes), i.e.,

$$\boldsymbol{s}_{\nabla_{\text{h}}\cdot} = \frac{1}{h^3}(0\ldots -1\ldots 0\ldots +1\ldots 0)^{\text{T}}. \tag{50}$$

Therefore, the adjoint field B_{adj} can be obtained by

$$B_{\text{adj}} = \boldsymbol{s}^{\text{T}}\boldsymbol{u}_{\text{adj}} = \boldsymbol{s}_J^{\text{T}}\boldsymbol{A}_{\text{adj}} + \boldsymbol{s}_{\nabla_{\text{h}}\cdot}^{\text{T}}\phi_{\text{adj}}. \tag{51}$$

As will being discussed in Section 5.1, the first term corresponds directly to the field due to wire current, and we can exclude it here. The second term is simply the potential difference at the two electrodes, i.e.,

$$\begin{aligned} \boldsymbol{s}_{\nabla_{\text{h}}\cdot}^{\text{T}}\phi_{\text{adj}} &= \frac{1}{h^3}(0\ldots -1\ldots 0\ldots +1\ldots 0)\phi_{\text{adj}} \\ &= \frac{1}{h^3}(\phi_{\text{adj}}^{+} - \phi_{\text{adj}}^{-}), \end{aligned} \tag{52}$$

where the superscript (+) and (−) denote the locations of the positive and negative electrodes, respectively. This shows that the adjoint field can also be expressed as

$$B_{\text{adj}} = \frac{1}{h^3}\int_0^H E_z^{\text{adj}}\,\text{d}z, \tag{53}$$

which is consistent with Eq. (8) in the reciprocity method (remember the magnetic moment here is h^3, which will cancel the term $1/h^3$ in Eq. (53))!

5. Implementation and numerical results

5.1. Implementation of adjoint method

In the previous sections, we have shown that both reciprocity and adjoint methods can be used to compute the magnetic field at a receiver. We prefer to use the adjoint method in the marine MMR case, because we can directly use our existing MMR code. Implementation of the Lorentz reciprocity method requires a 3-D frequency-domain EM code, which is computationally demanding. Below is the implementation of the adjoint algorithm, in the case that there are k transmitter bipoles and only one receiver. Three components of magnetic field are calculated at the receiver. Since the adjoint field B_{adj} is identical to the primal field B, we do not distinguish between them in the following derivation.

From Eq. (39), the x-component data at the receiver due to the first Tx, which is represented by a source vector $\boldsymbol{s}_1$, can be written as

$$B_x^1 = \boldsymbol{s}_1^{\text{T}}(\mathcal{A}^{\text{T}})^{-1}\boldsymbol{q}_x, \tag{54}$$

where $\boldsymbol{q}_x$ is the projection vector to generate the x-component from potentials, and superscript 1 in B_x^1 denotes the Tx number. Similarly, the y- and z-components are given by

$$B_y^1 = \boldsymbol{s}_1^{\text{T}}(\mathcal{A}^{\text{T}})^{-1}\boldsymbol{q}_y, \tag{55}$$

$$B_z^1 = \boldsymbol{s}_1^{\text{T}}(\mathcal{A}^{\text{T}})^{-1}\boldsymbol{q}_z. \tag{56}$$

Or we can tie them together as

$$\begin{pmatrix} B_x^1 \\ B_y^1 \\ B_z^1 \end{pmatrix} = \begin{pmatrix} s_1^T & \mathbf{0} & \mathbf{0} \\ \mathbf{0} & s_1^{\mathrm{T}} & \mathbf{0} \\ \mathbf{0} & \mathbf{0} & s_1^{\mathrm{T}} \end{pmatrix} \begin{pmatrix} (\mathcal{A}_1^{\mathrm{T}}) & \mathbf{0} & \mathbf{0} \\ \mathbf{0} & (\mathcal{A}_1^{\mathrm{T}}) & \mathbf{0} \\ \mathbf{0} & \mathbf{0} & (\mathcal{A}_1^{\mathrm{T}}) \end{pmatrix} \begin{pmatrix} \boldsymbol{q}_x \\ \boldsymbol{q}_y \\ \boldsymbol{q}_z \end{pmatrix} \tag{57}$$

For the rest of the $k-1$ Tx sources, we also have similar matrix equations, and we can put them together to form

$$\begin{pmatrix} B_x^1 \\ B_y^1 \\ B_z^1 \\ \vdots \\ B_x^k \\ B_y^k \\ B_z^k \end{pmatrix} = \begin{pmatrix} s_1^{\mathrm{T}} & \mathbf{0} & \mathbf{0} \\ \mathbf{0} & s_1^{\mathrm{T}} & \mathbf{0} \\ \mathbf{0} & \mathbf{0} & s_1^{\mathrm{T}} \\ \vdots & \vdots & \vdots \\ s_k^{\mathrm{T}} & \mathbf{0} & \mathbf{0} \\ \mathbf{0} & s_k^{\mathrm{T}} & \mathbf{0} \\ \mathbf{0} & \mathbf{0} & s_k^{\mathrm{T}} \end{pmatrix} \begin{pmatrix} (\mathcal{A}^{\mathrm{T}})^{-1} & \mathbf{0} & \mathbf{0} \\ \mathbf{0} & (\mathcal{A}^{\mathrm{T}})^{-1} & \mathbf{0} \\ \mathbf{0} & \mathbf{0} & (\mathcal{A}^{\mathrm{T}})^{-1} \end{pmatrix} \times \begin{pmatrix} \boldsymbol{q}_x \\ \boldsymbol{q}_y \\ \boldsymbol{q}_z \end{pmatrix} \tag{58}$$

Eq. (58) can also be written into a condensed form

$$\boldsymbol{B} = \boldsymbol{Q}_{\mathrm{adj}} \boldsymbol{u}_{\mathrm{adj}}, \tag{59}$$

where matrix $\boldsymbol{Q}_{\mathrm{adj}}$ is the first matrix on the right hand side of Eq. (58), and adjoint potential vector $\boldsymbol{u}_{\mathrm{adj}}$ can be obtained by solving the following adjoint equations

$$\begin{pmatrix} \mathcal{A}^{\mathrm{T}} & \mathbf{0} & \mathbf{0} \\ \mathbf{0} & \mathcal{A}^{\mathrm{T}} & \mathbf{0} \\ \mathbf{0} & \mathbf{0} & \mathcal{A}^{\mathrm{T}} \end{pmatrix} \boldsymbol{u}_{\mathrm{adj}} = \begin{pmatrix} \boldsymbol{q}_x \\ \boldsymbol{q}_y \\ \boldsymbol{q}_z \end{pmatrix} \tag{60}$$

which can be simplified as

$$\mathcal{A}_{\mathrm{adj}} \boldsymbol{u}_{\mathrm{adj}} = \boldsymbol{s}_{\mathrm{adj}}. \tag{61}$$

The coefficient matrix $\mathcal{A}_{\mathrm{adj}}$ in the adjoint method is related to the transpose of $\mathcal{A}$, and the adjoint source $\boldsymbol{s}_{\mathrm{adj}}$ is the projection vector. This clearly shows that we only need to solve the adjoint equations three times to obtain the adjoint potentials, and then compute the magnetic field by the inner product of the matrix $\boldsymbol{Q}_{\mathrm{adj}}$ and adjoint potentials. The number of the transmitters has little effect on the efficiency of the adjoint algorithm.

5.2. Numerical results

To verify the adjoint algorithm, we designed a 3-D model in the marine situation, as shown in Fig. 4. A 3-D conductive body, with dimensions of 2 km × 1 km × 1 km and conductivity of 1 S/m, is buried at depth of 500 m below the seafloor. The conductivities for the sea water and the medium below the sea floor are 3.3 and 0.1 S/m, respectively. There are 10 transmitter wires, running from the sea surface down to the seafloor, whose depth is 2500 m. One receiver is assumed to be positioned at (1, 0, and 0 km). The whole 3-D model, 21 km × 21 km × 21 km (including an 8.5 km

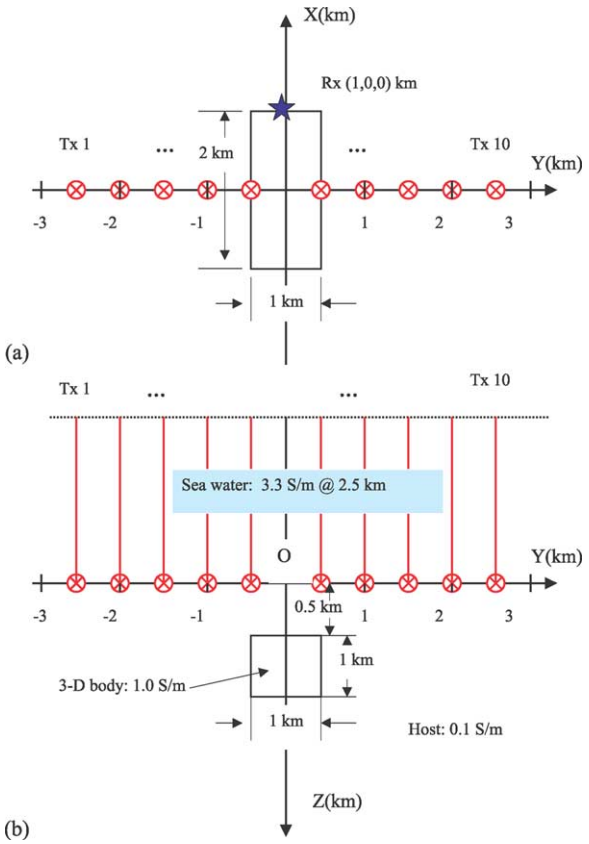

Fig. 4. A 3-D marine MMR model for testing the adjoint code. (a) The plan view; (b) the cross-section. Ten transmitters are uniformly deployed on both sides of the *y*-axis, with distances away from the origin: 2.5, 2.0, 1.5, 1.0, and 0.5 km. The receiver is located at (1, 0, and 0 km). Three components of magnetic field were computed for both the primal and adjoint cases. In addition, an integral equation-based code SYSEM was used to test the reciprocity for this model.

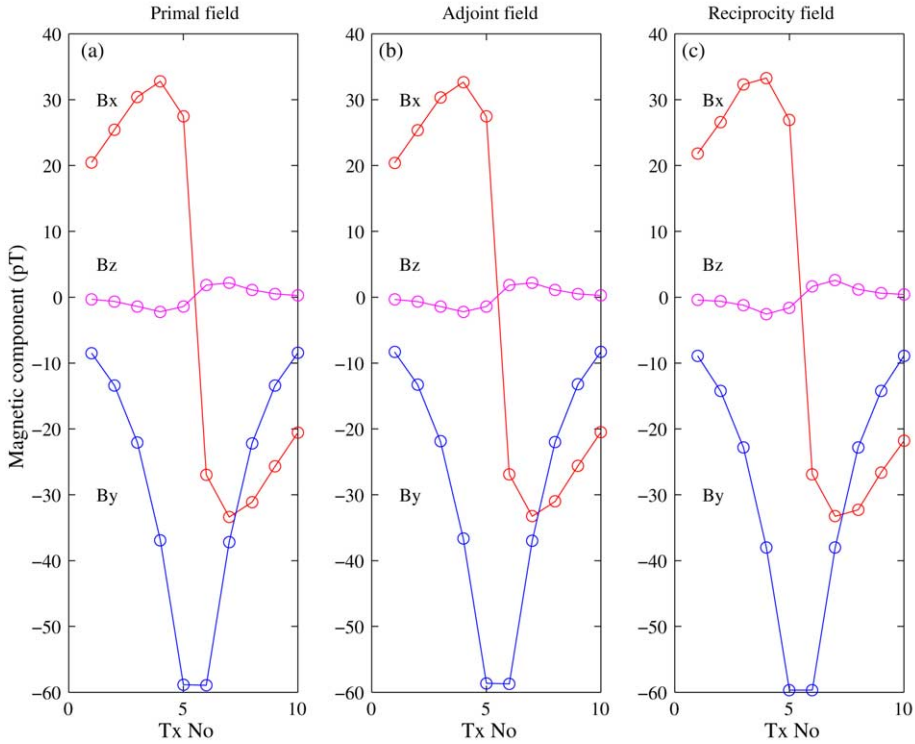

Fig. 5. Comparison of the primal, adjoint, and reciprocity solutions for the 3-D model shown in Fig. 4. The primal field (a) was obtained by running our 3-D MMR forward modelling code for each of the 10 transmitter wires. The adjoint field (b) was obtained by running our 3-D MMR adjoint code; and the reciprocity field (c) was from using SYSEM, in which three artificial magnetic dipoles (x-, y- and z-oriented in turn) were located at the Rx position. Then the magnetic field was computed using Eq. (8).

air layer in the vertical direction), was non-uniformly discretized into 83 km × 83 km × 77 km rectangular cells. The cell size ranged from 50 to 2000 m.

Since it is more accurate to compute the magnetic field due to the vertical wire using the Biot-Savart law, we excluded the term $\boldsymbol{J}^{\mathrm{s}}$ (no wire current) on the right hand side of Eq. (33), and only considered $\nabla_{\mathrm{h}} \cdot \boldsymbol{J}^{\mathrm{s}}$ (sources at the electrodes). This means the magnetic field computed in the 3-D code is only due to the current flow in the sea water and inside the sea floor. We ran the code twice. For the first run, we included all 10 Tx sources, directly solved Eq. (33), and obtained the magnetic field at the receiver. This field is called the primal field, and is shown in Fig. 5a. For the second run, we used the adjoint algorithm, solved Eq. (61), and obtained the adjoint field by Eq. (59). The results for the adjoint field are displayed in Fig. 5b. In addition, we ran another independent code SYSEM (Xiong, 1992), which is based on the integral equation method, to test the reciprocity relation as shown in Eq. (8). The artificial transmitter was a unit magnetic dipole, which was oriented to x-, y-, and z-direction in turn. The frequency was 0.001 Hz. We computed the vertical electric components E_z (imaginary part only) at an interval of 5 m along each Tx wire (from 0 to 2500 m). The total B field was obtained by integrating E_z along the wire and multiplying by $1/i\omega$. We then subtracted the magnetic field B^{w} due to the wire from the total B, and plotted the reciprocity fields in Fig. 5c. Generally these three methods produce results that agree quite well. The maximum relative error is less than 2.5%, which happens when the Tx is 2.7 km away from the receiver, and the signal is getting weaker: for example, B_y is reduced from 58.8 to 8.4 pT, and B_z is from 2.2 to 0.32 pT. For a large-scale numerical problem like this one, this error is reasonable and acceptable.

6. Discussion

We have demonstrated that both the Lorentz reciprocity and adjoint methods can be used to overcome the computational difficulty encountered when there are many transmitter sources but only a few receivers in the marine MMR problem. By using the Lorentz reciprocity, the magnetic field at a receiver, generated by a long transmitter wire, is exactly the same as the normalized electromotive force (or voltage) induced in the transmitter wire, generated by an artificial magnetic diploe located at the receiver position. To implement the Lorentz reciprocity, a 3-D frequency-domain EM code with a magnetic dipole source is needed. Numerically, we can set the frequency very low, say 0.001 Hz, and compute the normalized electromotive force. For our purposes it is more effective to use the adjoint method, since we are only required to solve a adjoint equation, in which the coefficient matrix $\mathcal{A}_{\text{adj}}$ is just a transpose of $\mathcal{A}$ in the primal problem. At the extreme limit when the frequency approaches zero, we have proved that the adjoint and reciprocity approaches have the same physical understanding: the artificial source is a magnetic dipole (or current loop) but with a steady current, while the "measurement" is the voltage induced along the transmitter wire.

The implementation of the adjoint method has been verified with a synthetic 3-D model, in which 10 transmitter sources and one receiver with three component magnetic field were involved. One comment we would like to make is about the efficiency of the adjoint code. In principle, the adjoint code should only take about one-third the computational time required in the primal problem (10 Txs versus three adjoint sources). In practice, the adjoint code in the above example was only two times faster than the primal code. After close inspection of the major computational steps, the time required can be attributed to: (1) forming the discrete operator matrices ∇_{h}, $\nabla_{\text{h}}\cdot$, $\nabla_{\text{h}}\times$, and the matrix $\mathcal{A}$ in Eq. (33); (2) solving Eq. (33) for potentials $\boldsymbol{u}$; (3) forming the projection matrix Q and obtaining $\boldsymbol{B}$ by multiplying Q by $\boldsymbol{u}$. When the scale of a 3-D modelling is not large, say the cell number is in the level of $30 \times 30 \times 30$, the time for step (1) and (3) might be negligible, compared to step (2). In that case, the computational time in the primal problem is dominated by solving the equation, and therefore is proportional to the number of the transmitter sources. When we deal with a large-scale problem, such as the $83 \times 83 \times 77$ in our test example, the time for steps (1) and (3) is significant, making the whole computational time no longer proportional to the number of the sources. This happened in our adjoint test example. However, in the EPR example mentioned at the beginning of the paper, use of the adjoint code will reduce the computational load to about one-tenth of the primal code (20 artificial sources versus 200 real sources). This reduction is crucial when we attempt to invert the EPR data. Implementation of the adjoint method in the 3-D inverse problem will be discussed in a subsequent paper.

Acknowledgments

We would like to thank Dr. K.H. Lee and Prof. M. Zhdanov for permission of using the code *EM1D* and *SYSEM*, respectively. *SYSEM* was developed at the Consortium for Electromagnetic Modelling and Inversion of the University of Utah. We are also grateful for the help from Dr. Oliver Dorn on the reciprocity by functional notation. Two reviewers, Professor M. Zhdanov and Dr. M. Everett, gave insightful comments on the original manuscript, prompting a much refined version. The work presented here was funded by NSERC and the "IMAGE" Consortium, of which the following are members: AGIP, Anglo American Corporation, BHP Billiton, EMI Inc., Falconbridge Ltd., INCO Exploration and Technical Services Inc.,Kennecott Exploration, MIM Exploration Pty. Ltd., Muskox Minerals Corp., Newmont Exploration Ltd., Placer Dome Inc., and Teck Cominco Ltd. We are grateful for their participation.

Appendix A. Four representations of reciprocity

In the EM geophysics, there exist two types of imposed sources: grounded wires (electric sources) and current loops (magnetic sources). The measurement is either an electric field (or voltage) and/or magnetic field. The various combinations of sources and receivers gives rise to four representations of recipocity.

A.1. Electric source—measuring voltage

In this case, the transmitter source and receiver are grounded bipoles. The magnetic current densities in Eq. (5) can be assumed to be zero ($\boldsymbol{M}^{\mathrm{a}}$, $\boldsymbol{M}^{\mathrm{b}} = 0$), and the electrical current densities can be represented as (Ward and Hohmann, 1988)

$$\boldsymbol{J}^{\mathrm{a}} = I^{\mathrm{a}}\delta(\boldsymbol{r} - \boldsymbol{r}_{\mathrm{a}})\,\mathrm{d}\boldsymbol{l}_{\mathrm{a}}, \tag{A.1}$$

$$\boldsymbol{J}^{\mathrm{b}} = I^{\mathrm{b}}\delta(\boldsymbol{r} - \boldsymbol{r}_{\mathrm{b}})\,\mathrm{d}\boldsymbol{l}_{\mathrm{b}}, \tag{A.2}$$

where I^{a} and I^{b} are the current strengths, $\boldsymbol{l}_{\mathrm{a}}$ and $\boldsymbol{l}_{\mathrm{b}}$ are the direction vectors of the unit current elements on the bipoles, and $\boldsymbol{r}_{\mathrm{a}}$ and $\boldsymbol{r}_{\mathrm{b}}$ are the location vectors. Substituting the electrical and magnetic current densities into Eq. (5) yields

$$I^{\mathrm{b}}\int_{l_{\mathrm{b}}} \boldsymbol{E}^{\mathrm{a}} \cdot \mathrm{d}\boldsymbol{l}_{\mathrm{b}} = I^{\mathrm{a}} \int_{l_{\mathrm{a}}} \boldsymbol{E}^{\mathrm{b}} \cdot \mathrm{d}\boldsymbol{l}_{\mathrm{a}}, \tag{A.3}$$

or

$$\frac{V^{\mathrm{a}}}{I^{\mathrm{a}}} = \frac{V^{\mathrm{b}}}{I^{\mathrm{b}}} \tag{A.4}$$

where V^{a} is the potential difference (or voltage) measured at the location b due to the bipole a; V^{b} is the voltage at the location a due to the bipole b. In the particular case when is, $I^{\mathrm{a}} = I^{\mathrm{b}}$, then

$$V^{\mathrm{a}} = V^{\mathrm{b}}. \tag{A.5}$$

This is the well-known reciprocity that is frequently used for DC surveys, in which the frequency used is eventually zero. It states, the potential difference between two electrodes (bipole **b**) when steady current is passing through another electrode pair (bipole **a**), is equal to that between bipole **a** if the same current is transmitted through bipole **b**, for any arbitrary conductivity distribution in the ground. Note that the reciprocity does not require the electrodes to be on the surface of the ground.

A.2. Electric source—measuring $\boldsymbol{B}$

The MMR method belongs to this category. Assume the transmitter is located at position a and the receiver at b. The electric and magnetic current densities can be set to

$$\boldsymbol{J}^{\mathrm{a}} = I^{\mathrm{a}}\delta(\boldsymbol{r} - \boldsymbol{r}_{\mathrm{a}})\,\mathrm{d}\boldsymbol{l}_{\mathrm{a}}, \quad \boldsymbol{M}^{\mathrm{a}} = 0, \tag{A.6}$$

and

$$\boldsymbol{J}^{\mathrm{b}} = 0, \quad \boldsymbol{M}^{\mathrm{b}} = i\omega\mu\boldsymbol{m}^{\mathrm{b}}\delta(\boldsymbol{r} - \boldsymbol{r}_{\mathrm{b}}), \tag{A.7}$$

where $\boldsymbol{m}^{\mathrm{b}}$ is the moment vector of an infinitesimal magnetic dipole. In practice, the magnetic dipole can be approximated by a small loop of current I^{b}, with loop area of s^{b}, i.e.,

$$\boldsymbol{m}^{\mathrm{b}} = \hat{\boldsymbol{u}} I^{\mathrm{b}} s^{\mathrm{b}}, \tag{A.8}$$

where $\hat{\boldsymbol{u}}$ is the unit vector normal to the loop area and is in the direction of the right-hand thumb if the fingers of the right-hand are curled in the direction of the current I^{b} circulating in the loop (right-hand rule). Putting the source terms into Eq. (5), will result in

$$\boldsymbol{B}^{\mathrm{a}} = \frac{\hat{\boldsymbol{u}} I^{\mathrm{a}}}{i\omega I^{\mathrm{b}} s^{\mathrm{b}}} \int_{l_{\mathrm{a}}} \boldsymbol{E}^{\mathrm{b}} \cdot \mathrm{d}\boldsymbol{l}_{\mathrm{a}}. \tag{A.9}$$

This means the $\boldsymbol{B}$ field at the receiver location due to a grounded wire source can be obtained by an integration of an $\boldsymbol{E}$ field along the grounded wire, then normalized by a factor related to angular frequency ω, current I^{a}, and magnetic moment m^{b} . The $\boldsymbol{E}$ field is generated by an artificial current loop source (or magnetic dipole) located at the receiver position. A simpler expression is arrived at by assuming $I^{\mathrm{a}} = 1$ and a unit magnetic dipole ($I^{\mathrm{b}} s^{\mathrm{b}} = 1$). By doing so, the above expression can be simplified as

$$\boldsymbol{B}^{\mathrm{a}} = \frac{\hat{\boldsymbol{u}}}{i\omega} \int_{l_{\mathrm{a}}} \boldsymbol{E}^{\mathrm{b}} \cdot \mathrm{d}\boldsymbol{l}_{\mathrm{a}}. \tag{A.10}$$

A.3. Magnetic source—measuring voltage

By setting appropriate electric and magnetic current densities, the voltage V^{a} at a receiver due to a magnetic source can be obtained by computing the magnetic field $\boldsymbol{B}^{\mathrm{b}}$ at a transmitter position, produced by an artificial grounded wire source located at the receiver, i.e.,

$$V^{\mathrm{a}} = \frac{i\omega\boldsymbol{m}^{\mathrm{a}} \cdot \boldsymbol{B}^{\mathrm{b}}}{I^{\mathrm{b}}}. \tag{A.11}$$

The representation is just reciprocal to Eq. (A.9). For a large loop source, we may divide it into many small loops and then sum up the voltage over each small loop by using (A.9).

A.4. Magnetic source—measuring $\boldsymbol{B}$

In this case, the electric current densities are set to zero, and only magnetic current sources are left. It is straightforward to derive

$$\boldsymbol{B}^{\mathrm{a}} \cdot \boldsymbol{m}^{\mathrm{b}} = \boldsymbol{B}^{\mathrm{a}} \cdot \boldsymbol{m}^{\mathrm{a}}. \tag{A.12}$$

It would be more intuitive to look at the reciprocity from the viewpoint of the complex electromotive force *emf*. Suppose the current $I^{\mathrm{a}} = I^{\mathrm{b}}$ in all the four cases. As we know, the *emf* can be defined as

$$\varepsilon^{E} = \int \boldsymbol{E} \cdot \mathrm{d}\boldsymbol{l} = V, \tag{A.13}$$

for an electrical source, and

$$\varepsilon^{M} = i\omega s B, \tag{A.14}$$

for a magnetic source, where s is the effective area of the magnetic loop. By using the *emf*, the reciprocity can be simplified as

$$\varepsilon^{\mathrm{a}} = \varepsilon^{\mathrm{b}}. \tag{A.15}$$

Therefore, the essence of the reciprocity is that the *emf* developed in a receiver, due to current flow in a transmitter, is exactly equal to the emf in a transmitter if the same current is flowing in a receiver.

Appendix B. Behavior of E field at low frequency

According to Méndez-Delgado et al. (1999), the electric field at low-frequency can be expanded in terms of Maclaurin power series, and can written as

$$\boldsymbol{E}(\boldsymbol{r}, \omega) = \boldsymbol{E}^{0}(\boldsymbol{r}) + \sum_{n=1}^{\infty} \left[\frac{1-(-1)^{n+1}}{2} + i\frac{1-(-1)^{n}}{2} \right] \times \boldsymbol{E}^{n}(\boldsymbol{r})\omega^{n}, \tag{B.1}$$

where $\boldsymbol{E}^{0}(\boldsymbol{r})$ represents the electric field at $\omega = 0$, and $\boldsymbol{E}^{n}(\boldsymbol{r})$ is the nth partial derivative of $\boldsymbol{E}$ with respect to ω evaluated at $\omega = 0$. So $\boldsymbol{E}^{1}(\boldsymbol{r}) = \partial \boldsymbol{E}(\boldsymbol{r}, \omega)/\partial\omega$ at $\omega = 0$. Note that $\boldsymbol{E}^{0}(\boldsymbol{r})$ and $\boldsymbol{E}^{n}(\boldsymbol{r})$ are now all real functions and independent of ω. When $\omega \longrightarrow 0$, we can neglect the terms associated with the second and higher order of powers, i.e.,

$$\boldsymbol{E}(\boldsymbol{r}, \omega) = \boldsymbol{E}^{0}(\boldsymbol{r}) + i\boldsymbol{E}^{1}(\boldsymbol{r})\omega. \tag{B.2}$$

For a magnetic loop source with static current ($\omega = 0$), the electric field $\boldsymbol{E}^{0}(\boldsymbol{r})$ anywhere in a general 3-D medium is zero ($\boldsymbol{E}^{0}(\boldsymbol{r}) = 0$), so we are left with

$$\boldsymbol{E}(\boldsymbol{r}, \omega) = i\omega\boldsymbol{E}^{1}(\boldsymbol{r}), \tag{B.3}$$

and $\boldsymbol{E}^{1}(\boldsymbol{r})$ is real, and can be calculated by solving a Fredholm integral equation of the second order

$$\boldsymbol{E}^{1}(\boldsymbol{r}) = \boldsymbol{E}^{1}_{p}(\boldsymbol{r}) + \int_{v'} G^{0}_{E}(\boldsymbol{r}, \boldsymbol{r}') \cdot \boldsymbol{E}^{1}(\boldsymbol{r}')\delta\sigma(\boldsymbol{r}')\,\mathrm{d}v', \tag{B.4}$$

where $\boldsymbol{E}^{1}_{p}(\boldsymbol{r})$ is the first order derivative, with respect to frequency, of the electric field in a uniform half-space of conductivity σ_0 due to a magnetic dipole source; $\boldsymbol{G}^{0}_{E}(\boldsymbol{r}, \boldsymbol{r}')$ is an electric dyadic Green's function in the homogeneous earth. Both $\boldsymbol{E}^{1}_{p}(\boldsymbol{r})$ and $\boldsymbol{G}^{0}_{E}(\boldsymbol{r}, \boldsymbol{r}')$ are given in analytic forms in the above mentioned paper. Therefore, $\boldsymbol{E}^{1}(\boldsymbol{r})$ is a constant factor only related to the geometry of the dipole source and receiver, not to the frequency.

Appendix C. Numerical tests of Eq. (6) in a 1-D medium

C.1. Analytical test

In Fig. C.1, a transmitter wire is laid vertically from the origin O (0 0 0) to point C(0 0 H) in a uniform whole space of constant conductivity σ. A steady current is passed through the wire, with current strength I^{a} and pointing downward. The observation point is assumed to be located at b ($0\,y\,z$) for simplicity. We now calculate the magnetic field directly and compare it with that obtained from reciprocity. In the direct way, we can derive an analytical expression for the magnetic field due to the transmitter wire in a whole space. Following the derivation of magnetic field within a layered earth excited by a point source (Edwards and Nabighian, 1991), an infinite vertical wire AO, carrying the excitation current I^{a} and terminating at the origin O, will generate

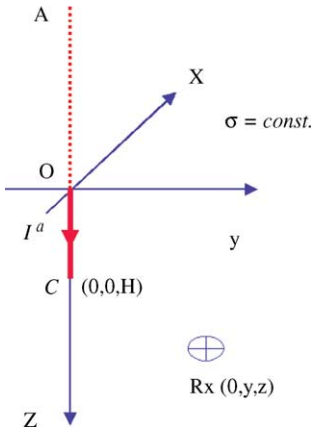

Fig. C.1. A simple whole space model for derivation of an analytical solution of a vertical wire bipole. The azimuthal magnetic field at receiver (0, *y*, *z*), due to the bipole, can be obtained by subtracting the magnetic field due to an infinite wire AO from and that due to infinite wire AOC.

an azimuthal magnetic field at the point b as

$$B_\phi^{\mathrm{AO}}(0,y,z)=\frac{\mu I^{\mathrm{a}}}{4\pi y}\left(1-\frac{z}{\sqrt{y^2+z^2}}\right). \tag{C.1}$$

Similarly, an infinite vertical wire AOC will produce

$$B_\phi^{\mathrm{AOC}}(0,y,z)=\frac{\mu I^{\mathrm{a}}}{4\pi y}\left(1-\frac{z-H}{\sqrt{y^2+(z-H)^2}}\right). \tag{C.2}$$

Therefore, the azimuthal magnetic field due to the wire OC can be obtained by subtracting B_ϕ^{AO} from B_ϕ^{AOC}, i.e.,

$$\begin{aligned}B_\phi^{\mathrm{OC}}(0,y,z)&=B_\phi^{\mathrm{AOC}}-B_\phi^{\mathrm{AO}}\\&=\frac{\mu I^{\mathrm{a}}}{4\pi y}\left(\frac{z}{\sqrt{y^2+z^2}}+\frac{H-z}{\sqrt{y^2+(H-z)^2}}\right).\end{aligned} \tag{C.3}$$

Note that the *x*-component B_x^{OC} at the observation point is opposite to B_ϕ^{OC}, i.e.,

$$\begin{aligned}B_x^{\mathrm{OC}}(0,y,z)&=-\frac{\mu I^{\mathrm{a}}}{4\pi y}\left(\frac{z}{\sqrt{y^2+z^2}}+\frac{H-z}{\sqrt{y^2+(H-z)^2}}\right).\end{aligned} \tag{C.4}$$

The other way is to use the reciprocity relation, which is given in Eq. (6). In order to use this relation, we have to put a *x*-oriented artificial magnetic dipole, with magnetic moment $m^{\mathrm{b}}=I^{\mathrm{b}}s^{\mathrm{b}}$, at the location b. The angular frequency ω is assumed to be very low. According to Ward and Hohmann (1988, p. 176, Eq. (2.56)), the vertical electric component E_z^{b} long the wire OC due to the magnetic dipole can be expressed as

$$E_z^{\mathrm{b}}(0,0,z')=\frac{i\omega\mu m^{\mathrm{b}}}{4\pi r^3}(ikr+1)e^{-ikr}y, \tag{C.5}$$

where wavenumber $k=\sqrt{\mu\epsilon\omega^2-i\omega\mu\sigma}$, and $r=\sqrt{y^2+(z-z')^2}$. When the frequency approaches to zero, $kr\to 0$, and $E_z^{\mathrm{b}}\to(i\omega\mu m^{\mathrm{b}}/4\pi r^3)y$. Note that the electric field varies as $i\omega$ as predicted earlier. Integration of vertical electric field along the wire yields

$$\int_0^H E_z^{\mathrm{b}}\,\mathrm{d}z'=\frac{i\omega\mu m^{\mathrm{b}}y}{4\pi}\int_0^H\frac{\mathrm{d}z'}{[y^2+(z-z')^2]^{3/2}} \tag{C.6}$$

$$=\frac{i\omega\mu m^{\mathrm{b}}}{4\pi y}\left(\frac{z}{\sqrt{y^2+z^2}}+\frac{H-z}{\sqrt{y^2+(H-z)^2}}\right). \tag{C.7}$$

After substituting Eq. (C.6) into Eq. (6), we have

$$\begin{aligned}B_x^{\mathrm{OC}}(0,y,z)&=-\frac{\mu I^{\mathrm{a}}}{4\pi y}\left(\frac{z}{\sqrt{y^2+z^2}}+\frac{H-z}{\sqrt{y^2+(H-z)^2}}\right),\end{aligned} \tag{C.8}$$

which is identical to Eq. (C.4), obtained through analytical derivations.

C.2. 1-D numerical test

As a simple numerical test, we use *EM1D*, a 1-D EM forward modelling code developed by Dr. K.H. Lee of University of California, Berkeley, to calculate the magnetic field due to an electric dipole, and then compare the magnetic field obtained by using the reciprocity relation in which the exciting source is a magnetic dipole. As shown in Fig. C.2, a *z*-oriented electric dipole is located at (0, 0, and 0.5 m), with current strength 1 A and dipole length 1 m. The receiver is at (0, 100, and 50 m). The conductivity of the uniform half-space is 0.01 S/m, and the frequency used is 0.001 Hz. The magnetic component H_x (real part) at receiver lo-

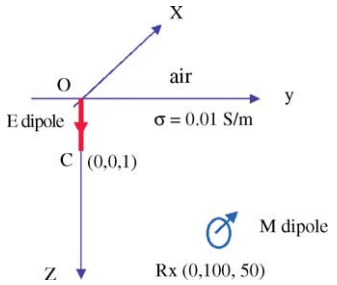

Fig. C.2. A simple half-space space model for numerical test of the reciprocity. A *z*-oriented unit electric dipole and a *x*-oriented unit magnetic dipole are located at (0, 0, and 0.5 m) and (0, 100, and 50 m), respectively. The conductivity of the half-space is 0.01 S/m, and the frequency used is 0.001 Hz. Code *EM1D* is used to do the comparison.

cation is -6.8330×10^{-8} A/m, computed by using the 1-D code. The imaginary part of H_x is negligible, six orders of magnitude less than its real counterpart.

Table C.1 lists the imaginary parts of vertical electric field E_z from (0, 0, amd 0 m) to (0, 0, 1 m), produced by a *x*-oriented unit magnetic dipole located at (0, 100, and 50 m). Approximating the integral of the E_z in Eq. (8) by summing up the values in Table C.1, and multiplying by an interval $\delta z_i'$ (=0.1), gives rise to

$$H_x(0, 100, 50) = \frac{1}{i\omega\mu}\int_0^1 E_z(0, 0, z')\,\mathrm{d}z' = \frac{1}{i\omega\mu}\sum_{i=1}^{10} E_i \delta z_i' = -6.8321 \times 10^{-8}. \quad \text{(C.9)}$$

Table C.1
The imaginary parts of the vertical electric field (V/m) at depth *z* varying from 0 to 1 along the wire

Depth *z* (m)	E_z (V/m)
0.01	-1.0808×10^{-17}
0.10	-1.0791×10^{-16}
0.20	-2.1582×10^{-16}
0.30	-3.2372×10^{-16}
0.40	-4.3162×10^{-16}
0.50	-5.3951×10^{-16}
0.60	-6.4739×10^{-16}
0.70	-7.5528×10^{-16}
0.80	-8.6316×10^{-16}
0.90	-9.7104×10^{-16}
1.00	-1.0789×10^{-15}

The generating source is a *x*-oriented unit magnetic dipole at (0, 100, and 50 m).

This value is very close to that computed directly from an electric dipole. The relative error between them is in the order of 0.01%.

References

Borcea, L., Papanicolaou, G., Tsogka, C., Berryman, J., 2002. Imaging and time reversal in random media. Inverse Problems 18, 1247–1279.

Chave, A.D., Constable, S.C., Edwards, R.N., 1991. Electrical exploration methods for the seafloor. In: Nabighian, M.N. (Ed.), Electromagnetic Methods in Applied Geophysics. Society of Exploration Geophysicists, Tulsa, Oklahoma, vol. 2, pp. 931–966.

Chen, J., Haber, E., Oldenburg, D.W., 2002. Three-dimensional numerical modelling and inversion of magnetometric resistivity data. Geophys. J. Int. 149, 679–697.

Dorn, O., Bertete-Aguirre, H., Berryman, J.G., Papanicolaou, G.C., 1999. A nonlinear inversion method for 3D electromagnetic imaging using adjoint fields. Inverse Problems 15, 1523–1558.

Edwards, R.N., Law, L.K., DeLaurier, J.M., 1985. On measuring the electrical conductivity of the oceanic crust by a modified magnetometric resistivity method. J. Geophys. Res. 86 B12, 11609–11615.

Edwards, R.N., Nabighian, M.N., 1991. The magnetometric resistivity method. In: Nabighian, M.N. (Ed.), Electromagnetic Methods in Applied Geophysics. Society of Exploration Geophysicists, Tulsa, Oklahoma, vol. 2, pp. 47–104.

Evans, R.L., Webb, S.C., Jegen, M., Sananikone, K., 1998. Hydrothermal circulation at the Cleft-Vance overlapping spreading center: results of a magnetometric resistivity survey. J. Geophys. Res. 103 B6, 12321–12338.

Evans, R.L., Webb, S.C., the RIFT-UMC Team, 2002. Crustal resistivity structure at 9°50′ N on the East Pacific rise: results of an electromagnetic survey, Geophys. Res. Letts., 29, 10.1029/2001GL014106.

Harrington, R.F., 1961. Time-Harmonic Electromagnetic Fields. McGraw-Hill, New York.

Haber, E., Ascher, U., 1943–1961. Fast finite volume modelling of 3D electro-magnetic problems with highly discontinuous coefficients: SIAM. J. Sci. Comput. 22.

Haber, E., Ascher, U.M., Aruliah, D., Oldenburg, D.W., 2000. Fast simulation of 3-D electromagnetic problems using potentials. J. Compd. Physics 163, 150–171.

Jin, J., 1993. The Finite Element Method in Electromagnetics. John Wiley and Sons, New York.

Madden, T.R., 1990. Inversion of low-frequency electromagnetic data. In: Desaubies, Y., Tarantola, A., Zinn-Justin, J. (Eds.), Oceanographic andgeophysical tomography. Elsevier Science Publishers B.V., North-Hollandm, pp. 377–408.

Mackie, R.L., Madden, T.R., 1993. Three-dimensional magnetotelluric inversion using conjugate gradients. Geophys. J. Int. 115, 215–219.

Méndez-Delgado, S., Gómez-Treviño, E., Pérez-Flores, M.A., 1999. Forward modelling of direct current and low-frequency electromagnetic fields using integral equations. Geophys. J. Int. 37, 336–352.

Marchuk, G.I., Agoshkov, V.I., Shutyaev, V.P., 1996. Adjoint equations and perturbation algorithms in nonlinear problems. CRC Press, Florida.

McGillivray, P.R., Oldenburg, D.W., Ellis, R.G., Habashy, T.M., 1994. Calculation of sensitivities for the frequency-domain EM problem. Geophys. J. Int. 116, 1–4.

Parasnis, D.S., 1988. Reciprocity theorems in geoelectric and geoelectromagnetic work. Geoexplanation 25, 177–198.

Ward, S.H., Hohmann, G.W., 1988. Electromagnetic theory for geophysical applications. In: Nabighian, M.N. (Ed.), Electromagnetic Methods in Applied Geophysics. Society of Exploration Geophysicists, Tulsa, Oklahoma, vol. 1, pp. 131–311.

Weidelt, P., 1975. Inversion of two-dimensional conductivity structures. Phys. EarthPlanet. Inter. 10, 281–291.

Xiong, Z., 1992. Electromagnetic modelling of 3D structures by the method of system iteration using integral equations. Geophysics 57, 1556–1561.

Zhdanov, M.S., 2002. Geophysical inverse theory and regularization problems. Elsevier, Amsterdam, New York, Tokyo.

Zhdanov, M.S., Frenkel, M.A., 1983. The solution of the inverse problems on the basis of the analytical continuation of the transient electromagnetic field in reverse time. J. Geomag. Geoelectr. 35, 747–765.

Zhdanov, M.S., Traynin, P., Booker, J., 1996. Underground imaging by frequency domain electromagnetic migration. Geophysics 61, 666–682.